This is a repository copy of *Shape coexistence and shape transition in self-conjugate nucleus 72Kr and the tensor force*.

White Rose Research Online URL for this paper:
https://eprints.whiterose.ac.uk/124299/

Version: Accepted Version

Article:
Kaneko, K., Sun, Y. and Wadsworth, R. orcid.org/0000-0002-4187-3102 (2017) Shape coexistence and shape transition in self-conjugate nucleus 72Kr and the tensor force. Physica Scripta. 114008. ISSN 0031-8949

https://doi.org/10.1088/1402-4896/aa8fdc

Reuse
Items deposited in White Rose Research Online are protected by copyright, with all rights reserved unless indicated otherwise. They may be downloaded and/or printed for private study, or other acts as permitted by national copyright laws. The publisher or other rights holders may allow further reproduction and re-use of the full text version. This is indicated by the licence information on the White Rose Research Online record for the item.

Takedown
If you consider content in White Rose Research Online to be in breach of UK law, please notify us by emailing eprints@whiterose.ac.uk including the URL of the record and the reason for the withdrawal request.

eprints@whiterose.ac.uk
https://eprints.whiterose.ac.uk/

Shape coexistence and shape transition in self-conjugate nucleus ^{72}Kr and the tensor force

K. Kaneko[a], Y. Sun[b,c,d], R. Wadsworth[e]

[a]Department of Physics, Kyushu Sangyo University, Fukuoka 813-8503, Japan
[b]Department of Physics and Astronomy, Shanghai Jiao Tong University, Shanghai 200240, China
[c]Collaborative Innovation Center of IFSA, Shanghai Jiao Tong University, Shanghai 200240, China
[d]Institute of Modern Physics, Chinese Academy of Sciences, Lanzhou 730000, China
[e]Department of Physics, University of York, Heslington, York YO 5DD, United Kingdom

Abstract

Oblate-prolate shape-coexistence is well-known in the $N = Z$ nucleus ^{72}Kr. Furthermore, recent experimental data implies that there is a rapid shape transition at very low spins in this nucleus. We reinvestigate this problem by using large-scale shell-model calculations with the monopole interactions derived from the monopole-based universal force that contains the tensor force in the Hamiltonian. We show that in ^{72}Kr, states with nucleon-quartet excitation from the pf shell to the $g_{9/2}$-$d_{5/2}$ orbits, which favor large prolate deformation, compete with those having the pf shell as the main configuration with oblate deformation. These shapes can coexist if the two types of states reside closely in excitation energy. In ^{72}Kr the tensor force is found to provide precisely such a coexistence condition near the ground state. As the tensor effect changes dynamically with orbital occupation when the nucleus rotates, a rapid shape transition can occur.

Keywords: Shape coexistence and transition, N = Z nuclei, Tensor force, Nucleon-quartet excitation, Large-scale shell model
PACS: 21.10.Sf, 21.30.Fe, 21.60.Cs, 27.50.+e

1. Introduction

The shape of a nucleus is an emergent phenomenon that results from the participation of many valence particles interacting via strong correlations. Coexistence of different shapes near the nuclear ground state is well known in various mass regions of the periodic table [1]. In nuclei, ground states with prolate deformation are found to be much more abundant than those with oblate deformation [2]. However, at or close to the $N = Z$ line in the mass region of $70 \leq A \leq 80$, two different shapes, with a strong prolate and a weak oblate deformation, can coexist [3]. Moreover, for proton/neutron numbers 34, 36, and 38, these shapes can change drastically as a function of spin and/or isospin [4]. ^{72}Kr, with the nucleon number $N = Z = 36$, is believed to form an acute example of a nucleus that changes shape with increasing spin. For example, it has been suggested by various theoretical calculations to have a predominantly oblate ground-state but with mixing of a prolate configuration at low excitation energies [4, 5, 6, 7, 8, 9, 10], and to undergo rapid shape changes with rotation. Already at spins $I = 4 - 6$, a robust prolate band was found to be developed [11, 12, 13], this occurs because when the nucleus rotates, particles in the fp shell are more easily excited to the deformation-driving $g_{9/2}$ orbit.

One important indication for shape coexistence in even-even nuclei is the observation of a second 0^+ state, 0_2^+ at low excitation energy, which may be interpreted as the ground state of a different shape. The 0_2^+ state in ^{72}Kr, with excitation energy 671 keV, was first observed [14] as a shape isomer and interpreted as the band-head of the known rotational structure with prolate deformation. Shape isomers [15] have generally very different structures from the ground state, and in the case of ^{72}Kr, it was suggested [16, 17] that its existence may have consequences for nucleosynthesis in the rapid-proton capture process [18]. Self-consistent deformed mean-field calculations have shown that shape coexistence takes place in Kr isotopes [19, 20, 21]. Later, in order to improve deficiencies of the single-particle spectra from the earlier calculation, the tensor field was included in the mean-field calculations [22, 23, 24, 25]. Beyond-mean-field calculations [26, 27, 28] were performed to understand the detailed structure of the shape isomer. Very recently, a large $E2$ transition rate, $B(E2; 4_1^+ \to 2_1^+)$, has been observed [29], which is 3.4 times larger than the previously reported $B(E2; 2_1^+ \to 0_1^+)$ rate [30]. This strongly suggests that the 0_1^+ state in ^{72}Kr does not belong to the same shape as the yrast 2_1^+ and 4_1^+ states, thereby providing an extreme example of a rapid shape transition near the ground state.

All the above works indicate that ^{72}Kr is located in a region of rapidly evolving nuclear shapes as a function of both spin and isospin. It is thus important to find the physical reasons that lead to these rapid dynamic changes. Through the studies of the neutron-rich nucleus ^{68}Ni, it has been recently suggested [31] that shell evolution can occur within the same nucleus through the combined effect of different major configurations and the

Email address: sunyang@sjtu.edu.cn (Y. Sun)

tensor force acting on them. The tensor force has been known to drive the shell evolution toward the exotic neutron-rich region [32], which could bring novel effects to binding energies and to spectra. The tensor driven monopole components are known to be remarkable for neutron-rich nuclei where the last protons and neutrons occupy different orbits. In ^{72}Kr, the last protons and neutrons occupy the same $f_{5/2}$ orbit and the tensor driven monopole terms give rise to a large repulsive interaction. We will show that for such self-conjugate nuclei the tensor force effect is significant and that in ^{72}Kr it could play a key role in changing the nuclear shape at low spin.

2. The shell-model framework

We have recently proposed [33] a unified realistic shell-model Hamiltonian called PMMU, consisting of the pairing+multipole Hamiltonian and the monopole interaction obtained by empirical fits to the monopole-based universal force [34]. It has been shown [33] that the PMMU model can be applied to the pf and $pf_{5/2}g_{9/2}$ (cited as pfg) shells. In Ref. [35], the model was systematically examined for the pfg shell nuclei by calculating various properties such as binding energies, energy levels, and electromagnetic transitions. However, for heavier $N \sim Z$ nuclei toward the mass-80 region, the $d_{5/2}$ orbit, which strongly couples with $g_{9/2}$ through large quadrupole matrix elements, will be important for the description of large deformation [36, 37, 38]. In the present work, we carry out shell-model calculations with the PMMU Hamiltonian in an enlarged model space $pf_{5/2}g_{9/2}d_{5/2}$ (cited as $pfgd$ hereafter). The single-particle (s.p.) energies and force strengths in the present work are adopted from our previous paper [35]. The low-lying states for the odd-mass nuclei in the fpg shell are described well in the fpg shell. Apart from single-particle (s.p.) energies and strength parameters in the PMMU model [33, 35], the $d_{5/2}$ s.p. energy is set to be 1.55 MeV higher than the $g_{9/2}$ orbit so as to reproduce the recent observed large $B(E2;4_1^+ \to 2_1^+)$ value [29] and the two-neutron shell gaps Δ for $Z = 31$ and 32, defined by $\Delta = S_{2n}(N = 52) - S_{2n}(N = 50)$ [39]. This new s.p. energy is close to 1.76 MeV chosen by Zuker *et al.* [40] so that the ground state band becomes solidly prolate. According to Ref. [40], the shell gap Δ varies as a function of orbital occupantions due to the monopole interaction, and the "monopole drift" determines the $d_{5/2}$ s. p. energy to be $2-3$ MeV above the $g_{9/2}$ orbit. Consequently, the shell gaps $\Delta = 3.5$ and 3.1 (in MeV), estimated from the experimental binding energies for $Z = 31$ and 32, are obtained.

Shell-model calculations have been performed with the code MSHELL64 [41]. For the $pfgd$ model space, however, the resulting dimension with exact calculation is huge. Therefore, the nucleon numbers n in the $g_{9/2}d_{5/2}$ (cited as gd hereafter) model space were restricted to $n \leq 4$. The spurious center-of-mass motion was not removed in the present calculation because the effects would be negligible [6].

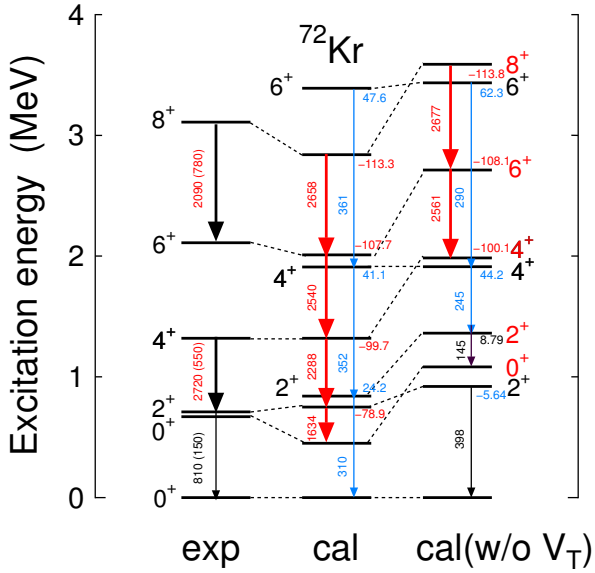

Figure 1: Energy levels, $B(E2)$ values, and spectroscopic quadrupole moments Q_s for ^{72}Kr. The $B(E2)$ and Q_s values are indicated by the numbers, in units of e^2fm^4 and $e$fm^2, respectively. The red and blue arrows indicate the $B(E2)$s that connect the states with negative and positive Q_s values, corresponding to prolate and oblate bands, respectively. Experimental data (left graph) are compared with the PMMU calculations with (mid graph) and without (right graph) the tensor force.

The PMMU Hamiltonian [33] is written as

$$H = H_0 + H_P + H_M + H_m, \quad (1)$$

$$H_0 = \sum_\alpha \varepsilon_a c_\alpha^\dagger c_\alpha,$$

$$H_P = -\sum_{J=0,2} \frac{1}{2} g_J \sum_{M\kappa} P_{JM1\kappa}^\dagger P_{JM1\kappa}$$

$$H_M = -\frac{1}{2}\chi_2 \sum_M : Q_{2M}^\dagger Q_{2M} : -\frac{1}{2}\chi_3 \sum_M : O_{3M}^\dagger O_{3M} :$$

$$H_m = \sum_{a\leq b,T} V_m(ab,T) \sum_{JMK} A_{JMTK}^\dagger(ab) A_{JMTK}(ab).$$

It includes the $J = 0$, 2 terms in the pairing channel and the quadrupole-quadrupole (QQ) and octupole-octupole (OO) terms in the multipole channel. We adopt the monopole matrix elements $V_m(ab,T)$ obtained by empirical fits to the monopole-based universal force V_{MU} [34], which contains the central force of a Gaussian form and the $\pi+\rho$ meson's exchange tensor force (denoted as V_T hereafter). In this way, the shell evolution is directly affected by the monopole interaction originating from the tensor force.

3. Results and discussion: Role of the tensor force

To understand the role of the tensor force, we have performed two sets of calculations for ^{72}Kr, with and without V_T, while all other calculation conditions remain the same. The level schemes obtained (mid and right graphs) are compared with experimental data (left graph) in Fig. 1. This figure shows also

Table 1: $B(E2)$ and Qs values for the positive-parity yrast states and some collective states of ^{72}Kr. Experimental data are taken from Ref. [11, 29].

	$B(E2)$ [e^{2}fm^4]			Q_s [efm^2]		
$J_i^\pi \to J_f^\pi$	exp	cal	cal(w/o V_T)	J_i^π	cal	cal(w/o V_T)
$2_1^+ \to 0_1^+$	810(150)	29	398	2_1^+	-78.9	-5.64
$4_1^+ \to 2_1^+$	2720(550)	2288	1	2_2^+	24.2	8.79
$6_1^+ \to 4_1^+$		2540	1	4_1^+	-99.7	44.2
$8_1^+ \to 6_1^+$	2090(780)	2658	2677	4_2^+	41.1	-100.1
$2_2^+ \to 0_1^+$		310	17	6_1^+	-107.7	-108.1
$2_1^+ \to 0_2^+$		1634	3	6_2^+	47.6	62.3
$2_2^+ \to 0_2^+$		60	145	8_1^+	-113.3	-113.8
$4_2^+ \to 2_2^+$		352	17			
$6_2^+ \to 4_2^+$		361	0			
$4_1^+ \to 2_2^+$		61	245			
$6_1^+ \to 4_2^+$		361	2561			
$6_2^+ \to 4_1^+$		0	290			

the $B(E2)$ values and spectroscopic quadrupole moments Q_s. In this mass region, the same effective charges as those used in Refs. [33, 35, 38, 42] are taken as $e_p = 1.5e$ and $e_n = 1.1e$. We note that these effective charges reproduce well the $B(E2)$ values over a wide range of the fpg-shell nuclei. It can be seen from the mid graph (labeled as 'cal') that the PMMU calculation with $V_{\rm T}$ obtains correctly a 0^+ as the first excited state. Furthermore, the other experimentally-known yrast states up to spin $I = 8$ are reproduced reasonably well. The second excited 2_2^+ state, not identified experimentally, is predicted to lie just above the 2_1^+ state. On top of the 2_2^+ state, the calculation predicts a 4_2^+ and a 6_2^+ state. The calculated Q_s for these states are listed in Fig. 1 with either a positive or a negative value, indicating that they are, respectively, oblate or prolate deformed. The red and blue arrows for two different rotational bands show the $B(E2)$ transitions, with the numerical value labeled on the arrows.

By comparing the calculations with and without the tensor force in Fig. 1 and Table 1, we see that the Q_s values for the 2_1^+ and 4_1^+ states and the $B(E2;4_1^+ \to 2_1^+)$ value are largely enhanced when the tensor force is switched on. Those states having large negative Q_s are connected by large $B(E2)$ values, corresponding to strong prolate-deformation. The calculation including the tensor force (see Fig. 1) suggests that the prolate states become yrast starting from $I = 2$. The calculated $B(E2;4_1^+ \to 2_1^+) = 2288$ e^2fm^4 is found to be in good agreement with the experimentally-determined value of 2720(550) e^2fm^4 [29] for this transition. As can be seen from 'cal' in Fig. 1, the calculated $B(E2;2_1^+ \to 0_2^+)$ is more than five times larger than $B(E2;2_2^+ \to 0_1^+)$. Furthermore, the ground 0_1^+ state is calculated to have positive Q_s value and the band built on it is connected by weaker $B(E2)$'s, which means oblate deformation. These results indicate that the ground 0_1^+ state does not belong to the same shape as the 2_1^+ state. The larger experimental value $B(E2;2^+ \to 0_1^+) = 810(150)e^2$fm^4 [29] may be understood by a mixture of oblate and prolate configurations resulting from enhanced excitations from the pf to the gd shells, which is supported by the conclusion in another recent study [10]. The limitation of our model space could be reason for the smaller theoretical $B(E2;2_1^+ \to 0_1^+)$ than the experimental one, while the $B(E2;4_1^+ \to 2_1^+)$ value is correctly reproduced. Thus, the present calculation for the oblate bandhead should be viewed as being qualitative rather than quantitative. All these experimental and theoretical results suggest that ^{72}Kr is a nucleus with oblate and prolate shapes coexisting at low excitation energy, which are mixed near the ground state.

When the tensor force is switched off in the calculation, (see in the right graph of Fig. 1 labeled as 'cal(w/o $V_{\rm T}$)', a qualitatively different picture is obtained. Comparing the mid and right graphs in this figure, we see two major differences. First, without $V_{\rm T}$, the calculated Q_s for the two 2^+ states have very small absolute values, corresponding to a near-spherical shape. There are no significant $B(E2)$ values for gamma decays coming from states up to the 4^+ level, suggesting that collective states characterized with certain shapes are not formed in the low spin region. This means that without the tensor force, the previously-discussed competing picture (up to 4^+) by the two shapes disappears. Furthermore, although the prolate band can still be formed, it appears at a much higher excitation region, inconsistent with the experimental data. Thus the calculation without the tensor part in the monopole-based universal force V_{MU} in (1) cannot describe the data.

We may understand the apparent differences between the 'cal' and 'cal(w/o $V_{\rm T}$)' results as follows. Since the monopole matrix element $V_m(f_{5/2}, f_{5/2}, T = 0)$ derived from the tensor force, which gives rise to the isoscalar neutron-proton pair correlation, is large and repulsive, the $f_{5/2}$ orbit is pushed up by this monopole term (as schematically shown in the insert to Fig. 2), which in turn reduces the $f_{5/2}$-$p_{1/2}$ energy gap when nucleons occupy the $f_{5/2}$ orbit. Thus, due to the tensor force, nucleons can be more easily excited from the $f_{5/2}$ orbit to the $p_{1/2}$ orbit. Figure 2 shows occupation numbers for the oblate (blue) and prolate (red) bands, with (solid) and without (dashed) $V_{\rm T}$ in the calculation, with calculated numbers listed in Table 2. For each case, the occupations are very similar for different spin states with $I = 0-6$ and hence several lines in Fig. 2 appear to bundle together. Proton and neutron occupation numbers in respective orbits are equal to each other for an $N = Z$ nucleus due

Table 2: Occupation numbers for ^{72}Kr, same for protons and neutrons, are displayed for the lowest four spins with $I = 0-6$. For each spin, the lowest two states are given, and their shapes (oblate or prolate) are determined based on the calculated sign of Q_s. For each orbit, the first (second) number corresponds to the result with (without) the tensor force.

	Oblate				Prolate			
Orbits	$I=0$	$I=2$	$I=4$	$I=6$	$I=0$	$I=2$	$I=4$	$I=6$
$p_{3/2}$	3.503	3.445	3.462	3.418	2.354	2.377	2.340	2.335
	3.374	3.247	3.315	3.209	2.196	3.335	2.192	2.186
$f_{5/2}$	2.707	2.712	2.728	2.789	3.187	3.170	3.176	3.178
	3.393	3.359	3.496	3.390	3.396	3.369	3.380	3.380
$p_{1/2}$	1.218	1.207	1.192	1.123	0.485	0.508	0.494	0.496
	0.734	0.827	0.648	0.800	0.427	0.770	0.440	0.442
$g_{9/2}$	0.314	0.339	0.322	0.334	1.176	1.156	1.185	1.215
	0.255	0.280	0.272	0.291	1.085	0.262	1.094	1.131
$d_{5/2}$	0.259	0.297	0.296	0.337	0.799	0.790	0.804	0.777
	0.243	0.287	0.268	0.309	0.896	0.263	0.894	0.861

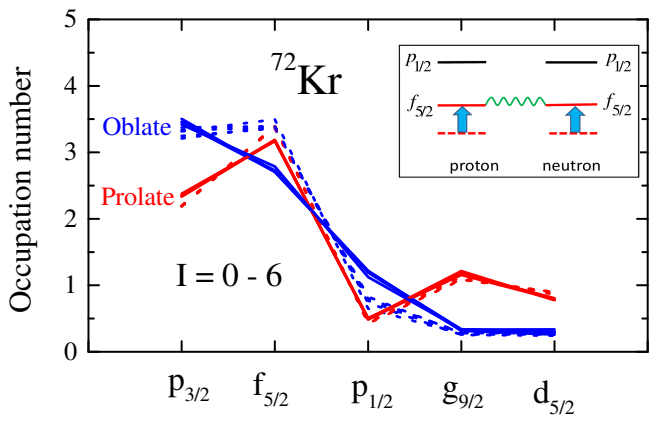

Figure 2: (Color online) Occupation numbers for ^{72}Kr, same for protons and neutrons. The solid (dashed) lines indicate occupation numbers calculated with (without) the tensor force. Red and blue lines are used to distinguish occupation numbers for the prolate and oblate bands shown in Fig. 1.

to conserved isospin. We first compare the occupation numbers for oblate and prolate bands with the tensor force. As seen from the solid blue curve in Fig. 2, nucleons in the oblate band largely involve pf shell configurations with negligible occupations in the gd shell. On the other hand, in the prolate band, the gd occupation is quite large and approximately two protons and two neutrons jump into the gd shell. Thus, it is considered that the large collectivity in the prolate band originates from the simultaneous excitations of two protons and two neutrons from the pf to gd shell. These quartet excitations will be discussed further in Section 4.. Such excitations have also been suggested for the interpretation of deformed bands in several $N = Z$ nuclei [45, 46, 47, 48].

When the tensor force is switched off, we find significant differences in occupation for the oblate band. As seen in Fig. 2, without $V_{\rm T}$, the occupation number of the $f_{5/2}$ ($p_{1/2}$) orbits increases (decreases) in the oblate band. Thus, due to the tensor force, the oblate band rises in energy because protons and neutrons in the $f_{5/2}$ orbit jump up to the $p_{1/2}$ orbit. The prolate band stays almost at the same energy because, as one sees from Fig. 2, the tensor force does not influence the occupations in the prolate band very much. In other words, relative to the oblate band, the prolate band is pushed down considerably due to the tensor force effect. For the two 2^+ states calculated without the tensor force, however, the occupation numbers (see Table 2) are small for the gd shell. This means that the protons and neutrons do not jump up from the pf to gd shell when the tensor force is switched off. As discussed above, the 2^+ states do not have large Q_s, and are not connected by strong $B(E2)$ values. When the tensor force is switched on, the quartet excitations from the pf to gd shell are clearly enhanced, which increases drastically the collectivity of the prolate states built on the first excited 0^+ state (see Fig. 1). We thus conclude that the apparent shape changes discussed in Fig. 1 can be explained by the enhanced excitation from the $f_{5/2}$ to the $p_{1/2}$ in the oblate configurations and that this is a direct consequence of the tensor force.

4. Further discussion: Excitation of nucleon quartets

The presence of shape phase transitions [49] is well known in nuclei in the high-spin region where spin-alignment occurs [50]. As already suggested in Ref. [37] and experimentally supported in Ref. [44], abrupt changes in structure happen when the proton and neutron numbers are near 35. In the present work, we further demonstrate that ^{72}Kr represents a unique example whereby the shape transition occurs within one nucleus due to excitation of nucleon quartets at very low spins. Figure 3 shows experimental data plotted in the form of spin I versus rotational frequency $\hbar\omega = [E(I) - E(I-2)]/2$ for several self-conjugate even-even nuclei from $N = Z = 32$ to 42. Note that for any given spin, ω is inversely proportional to moment of inertia defined as $\mathscr{J} = (I - 1/2)/\hbar\omega$. One sees a clear separation of two groups of data denoted by A ($N = Z > 36$) and B ($N = Z < 36$), indicating rather distinct shapes. The existing data for ^{72}Kr suggest that this $N = Z = 36$ nucleus lies at a very special position. It is seen that the data point for $I = 2$ of ^{72}Kr neither belongs to group A nor to group B, while those for $I = 4-8$ fall into group A. This is consistent with the shape mixing picture of the oblate and prolate configurations near the

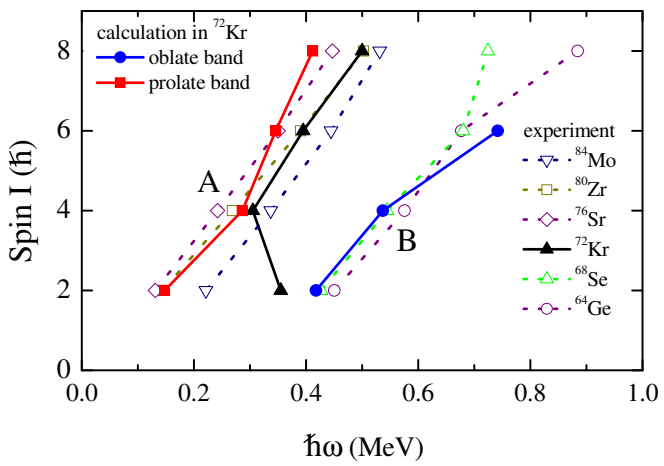

Figure 3: (Color online) Spin I versus the rotational frequency $\hbar\omega$. The experimental data are plotted for the even-even $N = Z$ nuclei with $A = 64 - 84$. The calculated results for the oblate and prolate bands in ^{72}Kr, shown in Fig. 1, are also plotted.

ground state. Our shell-model calculation for ^{72}Kr finds that the two $I = 2$ states fall in to the group A and B, respectively. Qualitatively, this indicates that there may be insufficient mixing in our calculations to replicate the properties of the yrast 2^+ state, as already discussed earlier. However, a larger $\mathscr{J}$ in the group A for the prolate band signifies a larger collectivity, which is consistent with the $B(E2)$ and Q_s results discussed in Fig. 1.

Shape coexistence in nuclei had its historical examples [1] in the neighborhood of the $N = Z$ isotopes ^{16}O, ^{40}Ca, and ^{56}Ni, which are all α-particle multiplets. The high binding-energy of the α-particle could make it energetically favorable for nucleon quartets [51] (comprising two protons and two neutrons) to form within the nucleus. Projected Shell Model [52] calculations for the $N = Z$ nuclei ^{48}Cr [45] and ^{36}Ar [46] showed that along the yrast band, the excitation of nucleon quartets is the most favorable mode when these nuclei rotate [48]. Independently, Xu *et al.* [53] have recently found that such a quartetting wave function is dominant for the α-cluster preformation in dynamic processes of radioactive α-decay. Remarkably, the states belonging to the group A in Fig. 3 clearly differ to those in B by excitations of nucleon quartets from the pf shell to the $g_{9/2}$-$d_{5/2}$ orbits. In the transitional nucleus ^{72}Kr, the states with nucleon-quartet excitation compete with those having only pf orbital occupation. The phenomenon of shape-coexistence may occur if the two types of states reside at similar energies at a given spin. Our calculations suggest that here the tensor force plays a role in setting up a shape co-existence environment near the ground state, without which the two types of states would have a greater separation energy (see Fig. 1). The tensor effect changes dynamically with spin and orbital occupation. In ^{72}Kr, the consequence of the competition shows up as a dramatic shape transition at $I = 2$ on the yrast line.

5. Summary

To summarize, the phenomenon of oblate-prolate shape-coexistence in ^{72}Kr is well known, but a deeper understanding for this problem at the interaction level has been missing. In order to learn about the physical origin, we have reinvestigated this problem by performing large-scale shell-model calculations using the PMMU interaction in the $pfgd$ model space. The monopole interactions derived from the monopole-based universal force that contains the tensor force are explicitly included in the Hamiltonian, and the role in the shape evolution in self-conjugate nuclei can thus be discussed. By comparing the calculations with and without the tensor force, we found key differences between the two calculations in terms of the particle occupations in particular orbits. We thus conclude that shell evolution can occur within the same nucleus through the combined effects of participating orbits and the tensor force acting on them. Shapes can coexist if two kinds of states, one with large prolate deformation and the other with weak oblate deformation, are found to be near the ground state. In ^{72}Kr, the structure difference between the two kinds of states is a nucleon-quartet excitation from the pf shell to the $g_{9/2}$-$d_{5/2}$ orbits. Moreover, it is the tensor force that creates a dynamical competition environment, in which a shape transition can happen at very low spins. However, as our employed $d_{5/2}$ s. p. energy (1.55 MeV above the $g_{9/2}$ orbit) is low compared to the value used in Ref. [40], further investigation to determine the $d_{5/2}$ s. p. energy in this region is desired.

A remaining question is how to understand the fact that various beyond-mean-field calculations are able to describe, to a reasonable extent, the oblate-prolate shape coexistence phenomena in this mass region without explicit inclusion of the tensor force. We believe that this question is more fundamental, and a definite answer lies beyond the scope of the present paper. It is well-known that the tensor force is a key ingredient in the nucleon-nucleon bare interaction, and is explicitly included in the shell-model interaction for the Hamiltonian constructed from first principles. It has been long realized that in this mass region, the mean-field single-particle energies are very different from the data, and thus from the shell-model single-particle energies if those are taken directly from the data [54]. We thus speculate that the tensor effect must be hidden in the mean-field approaches, even though the term does not explicitly appear, so that their success in dealing with shape changes and shape coexistence can be explained. However, a derivation from the first principle is still lacking. On the other hand, the effect of the tensor field in the mean-field approaches on the deformation [21] and on Gamow-Teller transitions [55, 56] has been investigated, providing examples of explicitly including this force in mean-field models to describe some particular quantities.

Acknowledgments

Research at SJTU was supported by the National Natural Science Foundation of China (No. 11575112), the 973 Program of China (No. 2013CB834401), and the National Key Research

and Development Program (No. 2016YFA0400501), and at York by the UK STFC under grant number ST/L005727/1.

References

[1] K. Heyde and J. L. Wood, Rev. Mod. Phys. **83** (2011) 1467.
[2] N. Tajima and N. Suzuki, Phys. Rev. C **64** (2001) 037301.
[3] S. M. Fischer *et al.*, Phys. Rev. Lett. **84** (2000) 4064.
[4] M. Yamagami, K. Matsuyanagi, M. Matsuo, Nucl. Phys. A **693** (2001) 579.
[5] A. Petrovici, K. W. Schmid, and A. Faessler, Nucl. Phys. A **665** (2000) 333.
[6] A. Petrovici, K. W. Schmid, and A. Faessler, Nucl. Phys. A **708** (2002) 190.
[7] D. Almehed and N. R. Walet, Phys. Lett. B **604** (2004) 163.
[8] T. A. War, R. Devi, and S. K. Khosa, Eur. Phys. J. A **22** (2004) 13.
[9] M. Bender, P. Bonche, and P.-H. Heenen, Phys. Rev. C. **74** (2006) 024312.
[10] J. A. Briz *et al.* Phys. Rev. C **92** (2015) 054326.
[11] G. de Angelis *et al.*, Phys. Lett. B **415** (1997) 217.
[12] N. S. Kelsall *et al.*, Phys. Rev. C **64** (2001) 024309.
[13] S. M. Fischer, C. J. Lister, and D. P. Balamuth, Phys. Rev. C **67** (2003) 064318.
[14] E. Bouchez *et al.*, Phys. Rev. Lett. **90** (2003) 082502.
[15] P. M. Walker and G. D. Dracoulis, Nature (London) **399** (1999) 35.
[16] Y. Sun, M. Wiescher, A. Aprahamian, and J. Fisker, Nucl. Phys. A **758** (2005) 765c.
[17] A. Petrovici and O. Andrei, Eur. Phys. J. A **51** (2015) 133.
[18] H. Schatz *et al.*, Phys. Rep. **294** (1998) 167.
[19] P. Sarriguren, E. Moya de Guerra, and A. Escuderos, Nucl. Phys. A **658**, (1999) 13.
[20] P. Sarriguren, E. Moya de Guerra, A. Escuderos, and A.C. Carrizo, Nucl. Phys. A **635**, (1998) 55.
[21] P. Sarriguren, E. Moya de Guerra, and A. Escuderos, Phys. Rev. C **64**, (2001) 064306.
[22] T. Otsuka, T. Matsuo, and D. Abe, Phys. Rev. Lett. **97** (2006) 162501.
[23] M. Zalewski, J. Dobaczewski, W. Satula, and T. R. Werner, Phys. Rev. C *bf*77, (2014) 024316.
[24] M. Zalewski, P. Olbratowski, M. Rafalski, W. Satula, T. R. Werner, and R. A. Wyss, Phys. Rev. C *bf*80, (2009) 064307.
[25] M. Bender, K. Bennaceur, T. Duguet, P.-H. Heenen, T. Lesinski, and J. Meyer, Phys. Rev. C **80**, (2009) 064302.
[26] A. Petrovici, K. W. Schmid, A. Faessler, Prog. Part. Nucl. Phys. **38** (1997) 161.
[27] K. Sato and N. Hinohara, Nucl. Phys. A **849** (2011) 53.
[28] Y. Fu *et al.*, Phys. Rev. C **87** (2013) 054305.
[29] H. Iwasaki *et al.*, Phys. Rev. Lett. **112** (2014) 142502.
[30] A. Gade, *et al.*, Phys. Rev. Lett. **95** (2005) 022502.
[31] Y. Tsunoda *et al.*, Phys. Rev. C **89** (2014) 031301(R).
[32] T. Otsuka *et al.*, Phys. Rev. Lett. **95** (2005) 232502.
[33] K. Kaneko, T. Mizusaki, Y. Sun, and S. Tazaki, Phys. Rev. C **89** (2014) 011302(R).
[34] T. Otsuka *et al.*, Phys. Rev. Lett. **104** (2010) 012501.
[35] K. Kaneko, T. Mizusaki, Y. Sun, and S. Tazaki, Phys. Rev. C **92** (2015) 044331.
[36] M. Hasegawa, K. Kaneko, T. Mizusaki, and S. Tazaki, Phys. Rev. C **69** (2004) 034324.
[37] M. Hasegawa, K. Kaneko, T. Mizusaki, and Y. Sun, Phys. Lett. B **656** (2007) 51.
[38] K. Kaneko, Y. Sun, and G. de Angelis, Nucl. Phys. A, **957** (2017) 144.
[39] J. Hakala *et al.*, Phys. Rev. Lett. **101** (2008) 052502.
[40] A. P. Zuker, A. Poves, F. Nowacki, and S. M. Lenzi, Phys. Rev. C **92** (2015) 024320.
[41] T. Mizusaki, N. Shimizu, Y. Utsuno, and M. Honma, code MSHELL64 (unpublished).
[42] M. Honma, T. Otsuka, T. Mizusaki, and M. Hjorth-Jensen, Phys. Rev. C **80** (2009) 064323.
[43] J. Ljungvall *et al.*, Phys. Rev. Lett. **100** (2008) 102502.
[44] A. J. Nichols *et al.*, Phys. Lett. B **733** (2014) 52.
[45] K. Hara, Y. Sun, and T. Mizusaki, Phys. Rev. Lett. **83** (1999) 1922.
[46] G.-L. Long and Y. Sun, Phys. Rev. C **63** (2001) 021305(R).
[47] T. Mizusaki, T. Otsuka, M. Honma, and B. A. Brown, Phys. Rev. C **63** (2001) 044306.
[48] Y. Sun, Phys. Scr. **91** (2016) 043005.
[49] F. Iachello, N. V. Zamfir, R. F. Casten, Phys. Rev. Lett. **81** (1998) 1191.
[50] Y. Sun, P. M. Walker, F.-R. Xu, and Y.-X. Liu, Phys. Lett. B **659** (2008) 165.
[51] M. Freer, Nature (London) **487** (2012) 309.
[52] K. Hara and Y. Sun, Int. J. Mod. Phys. E **4** (1995) 637.
[53] C. Xu *et al.*, Phys. Rev. C **95** (2017) 061306(R).
[54] Y. Sun, J.-y. Zhang, M. Guidry, J. Meng, and S. Im, Phys. Rev. C **62** (2000) 021601(R).
[55] C. L. Bai *et al.*, Phys. Rev. Lett. **105** (2010) 072501.
[56] F. Minato and C. L. Bai, Phys. Rev. Lett. **110** (2013) 122501.